AD
Reports Control Symbol
OSD-1366

RESEARCH AND DEVELOPMENT TECHNICAL REPORT
ECOM-5416

WIND TUNNEL SIMULATION AND PROTOTYPE STUDIES OF BARRIER FLOW PHENOMENA

By

J. D. Horn

G. S. Campbell

A. L. Wallis
Capt., USAF, Holloman Air Force Base

R. G. McIntyre
University of Texas at El Paso

December 1971

ECOM

UNITED STATES ARMY ELECTRONICS COMMAND - FORT MONMOUTH, NEW JERSEY

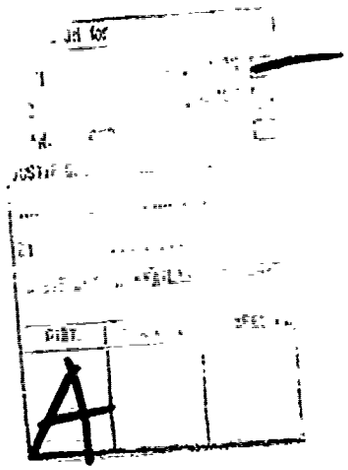

NOTICES

Disclaimers

The findings in this report are not to be construed as an official Department of the Army position, unless so designated by other authorized documents.

The citation of trade names and names of manufacturers in this report is not to be construed as official Government indorsement or approval of commercial products or services referenced herein.

Disposition

Destroy this report when it is no longer needed. Do not return it to the originator.

Reports Control Symbol
OSD-1366

Technical Report ECOM-5416

WIND TUNNEL SIMULATION AND PROTOTYPE STUDIES OF BARRIER FLOW PHENOMENA

By

J. D. Horn

G. S. Campbell

A. L. Wallis
Capt., USAF, Holloman Air Force Base

R. G. McIntyre
University of Texas at El Paso

Atmospheric Sciences Laboratory
White Sands Missile Range, New Mexico

December 1971

DA Project No. 1T062111A126

U. S. Army Electronics Command

Fort Monmouth, New Jersey

UNCLASSIFIED
Security Classification

DOCUMENT CONTROL DATA - R & D

(Security classification of title, body of abstract and indexing annotation must be entered when the overall report is classified)

1. ORIGINATING ACTIVITY (Corporate author)
Atmospheric Sciences Laboratory
White Sands Missile Range, New Mexico

2a. REPORT SECURITY CLASSIFICATION
Unclassified

2b. GROUP

3. REPORT TITLE
WIND TUNNEL SIMULATION AND PROTOTYPE STUDIES OF BARRIER FLOW PHENOMENA

4. DESCRIPTIVE NOTES (Type of report and inclusive dates)

5. AUTHOR(S) (First name, middle initial, last name)
J. D. Horn, G. S. Campbell, A. L. Wallis, R. G. McIntyre

6. REPORT DATE
December 1971

7a. TOTAL NO. OF PAGES
33

7b. NO. OF REFS
18

8a. CONTRACT OR GRANT NO.

b. PROJECT NO. 1T062111A126

c.

d.

9a. ORIGINATOR'S REPORT NUMBER(S)
ECOM-5416

9b. OTHER REPORT NO(S) (Any other numbers that may be assigned this report)

10. DISTRIBUTION STATEMENT
Approved for public release; distribution unlimited.

11. SUPPLEMENTARY NOTES
Details of illustrations in this document may be better studied on microfiche

12. SPONSORING MILITARY ACTIVITY
U. S. Army Electronics Command
Fort Monmouth, New Jersey

13. ABSTRACT

Design criteria were sought for a wind barrier to be erected along the 1.8-km rain erosion test section of the Rocket Sled Test Track located at Holloman Air Force Base, New Mexico. Simulated rainfall at the test facility is highly sensitive to cross-wind components, particularly those exceeding one m/s. Research on wind barrier configurations to provide protection for the test track rainfield includes both wind tunnel and prototype studies. Results obtained with a prototype barrier in the open atmosphere and wind tunnel simulation models at scaling ratios of 1:3 and 1:40, gave wind defects (effective percentage decrease of wind speed over the critical area) of 70% or more for an optimum barrier design of 35% permeability based on measurements taken at a horizontal distance equal to 2-3 barrier heights downstream of the barrier. A barrier design is proposed which would markedly increase the number of days during which the wind-sensitive rain field simulation facility of the test track could be successfully used. As a result of the tests specific recommendations are made for a 6m high barrier of 35% hole area to be located parallel to the rain field test area and displaced 15m to the west.

DD FORM 1 NOV 68 1473 REPLACES DD FORM 1473, 1 JAN 64, WHICH IS OBSOLETE FOR ARMY USE.

UNCLASSIFIED
Security Classification

14. KEY WORDS	LINK A		LINK B		LINK C	
	ROLE	WT	ROLE	WT	ROLE	WT
1. Wind reduction 2. Wind barrier 3. Shelter belt						

ABSTRACT

Design criteria were sought for a wind barrier to be erected along the 1.8 km rain erosion test section of the Rocket Sled Test Track located at Holloman Air Force Base, New Mexico. Simulated rainfall at the test facility is highly sensitive to cross-wind components, particularly those exceeding one m/s.

Research on wind barrier configurations to provide protection for the test track rainfield includes both wind tunnel and prototype studies. Results obtained with a prototype barrier in the open atmosphere and wind tunnel simulation models at scaling ratios of 1:3 and 1:40 gave wind defects (effective percentage decrease of wind speed over the critical area) of 70% or more for an optimum barrier design of 35% permeability based on measurements taken at a horizontal distance equal to 2-3 barrier heights downstream of the barrier.

A barrier design is proposed which would markedly increase the number of days during which the wind-sensitive rain field simulation facility of the test track could be successfully used. As a result of the tests specific recommendations are made for a 6m high barrier of 35% hole area to be located parallel to the rain field test area and displaced 15m to the west.

CONTENTS

INTRODUCTION

The Rocket Sled Test Track located at Holloman Air Force Base, a supplemental area of White Sands Missile Range (WSMR), New Mexico, is a facility for the testing of rain erosion on supersonic projectiles moving along a 1.8 km erosion test section. The artificially produced rain field, however, can be excessively distorted by winds with transverse components in excess of one meter per second. This condition prevails about 35% of the time. However, the transverse component of wind speed is less than three meters per second only about 85% of the time. Therefore, a wind barrier reducing the transverse component of wind from three meters per second to a value of one meter per second will more than double the number of days per year in which the test facility may be used. Because of the high cost of manning the test facility, the monetary loss due to "scrubbed" tests is many thousands of dollars per month. Therefore, a properly designed barrier will result in very great savings to the government.

This study considers the design features necessary to construct a wind barrier. Models were constructed and tested in the Atmospheric Sciences Laboratory wind tunnel at WSMR. Prototype models were then constructed and field tested. Finally, recommendations are given concerning the design and construction of the needed wind barrier at the rocket sled test facility.

BACKGROUND

The utility of wind barriers has been recognized for many years. Agricultural scientists have used the shelter effect of semidense rows of trees planted upwind (to the prevailing wind) of a cultivated area to reduce wind damage to crops substantially. Snow fences have been used along roads (depositing snow before it reaches the road) and in mountain areas (settling vastly greater amounts of snow to increase summertime water run-off).

The adaptation of natural barriers is mentioned by Geiger [1] and Sutton [2]. Early quantitative work was undertaken by Jensen [3], who performed the task of obtaining accurate wind defect data.

Geiger refers to Nägeli's work [4] on the pattern of wind defect behind a 2.2 m screen of 45-55% hole area (Figure 1). The zone of maximum protection for this configuration lies at a horizontal distance equal to 4 to 5 barrier heights (bh) downstream, while a 50% wind reduction is observed for as far as 12 bh at approximately 1/2 bh above the ground. Figure 2 shows the relative effect of shelter belt density from which it is apparent that the most dense barrier provides maximum protection

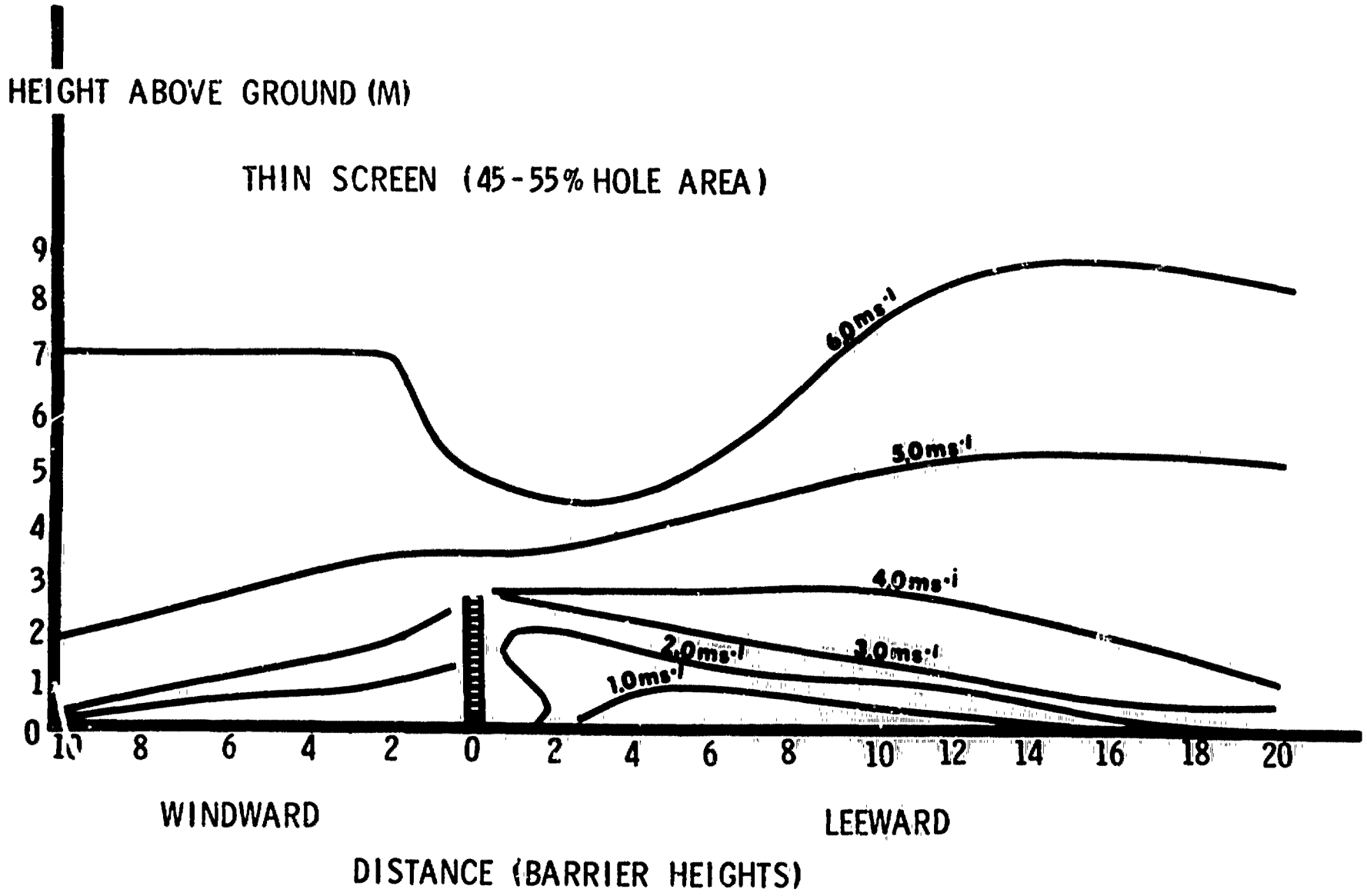

Figure 1. Wind field around reed screen (from measurements made by Nägeli [4]).

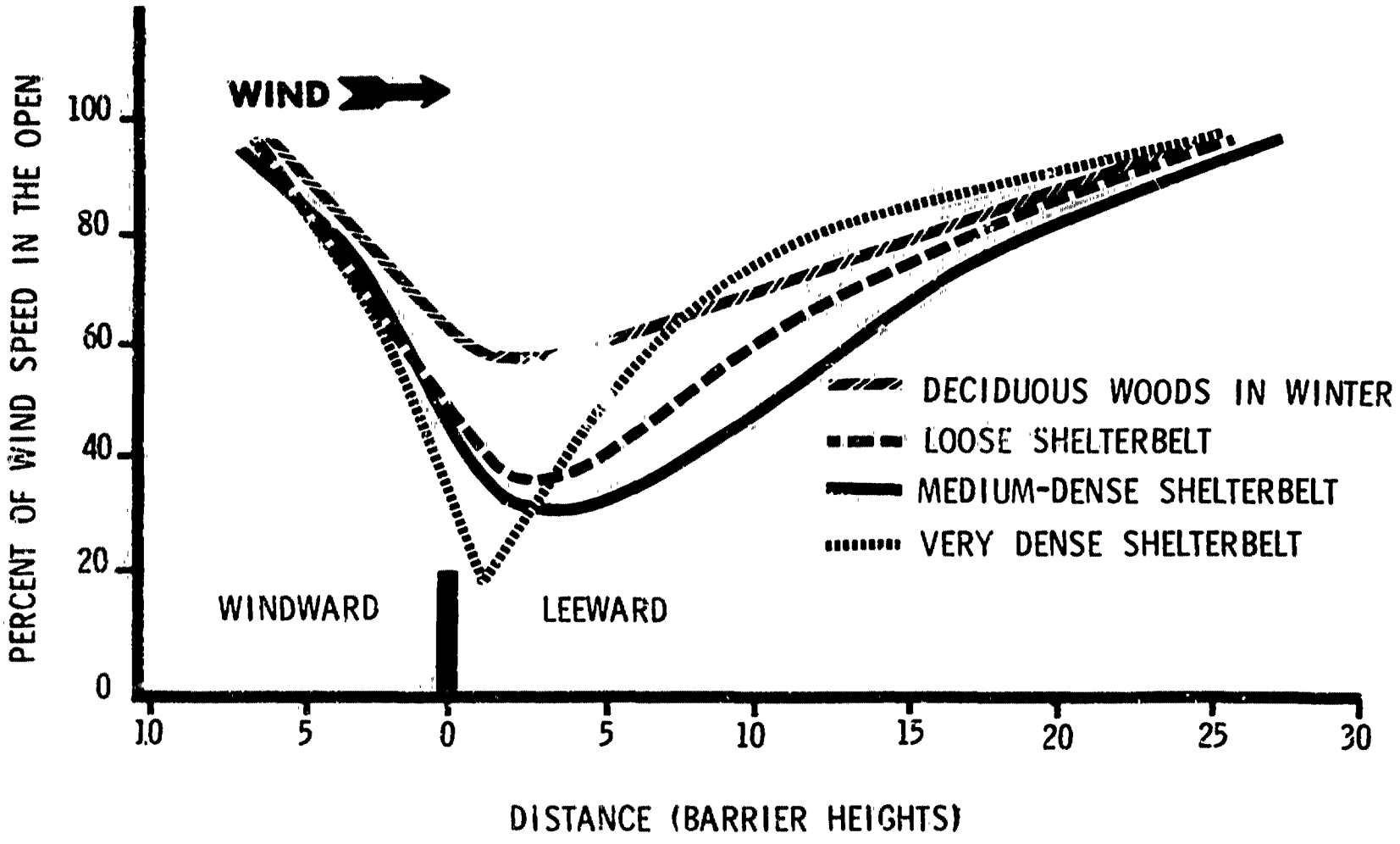

Figure 2. Shelter effect as a function of permeability (based on measurements made by Nägeli [5]).

immediately behind the obstacle (with higher turbulence levels in the protection region) at about 1 bh, but that a medium-dense shelter belt affords wind defect amounts up to 65% some 4 bh downstream.

THEORETICAL CONSIDERATIONS

The flow phenomenon may be considered as a steady mean current with superimposed perturbations over a wide range of scales. If we consider the barrier as a wall with a half cylinder at the top, we know that the onset of turbulence downstream from the barrier will occur in a time directly proportional to the radius of the cylinder. Therefore, in the limiting case of zero radius, the onset is practically instantaneous regardless of flow velocity.

Ideally the steady flow should yield to a theoretical treatment by writing down flow equations, representing the differential equations by difference equations and programming their appropriate numerical solutions on an adequately fast and large computer subject to the appropriate boundary and initial conditions. However, the singularity introduced by the projecting edge of the barrier causes standard routine methods of solution to break down and forces introduction into the problem of an approximate boundary condition, e.g., a small-radius cylinder at the top, and changes the very nature of the barrier.

In addition, the treatment of turbulence requires the introduction of empirical functions appropriate to the regime under consideration. Unfortunately, every such empirical function contains certain parameters which can be evaluated only by experimental studies. Such procedures might be worthwhile if one needed a guide for designing barriers for a number of applications with very precise design specifications imposed. However, by the time a prototype barrier is built and experimental studies are made and compared with wind tunnel results, all the necessary information is available for the design of an effective barrier for the Holloman facility. Any inclusion of empirical functions to demonstrate a more precise mathematical analysis would not add materially to the content of the paper. In no practical application of wind barriers has a mathematical analysis been fruitful because of the very nature of the singular boundary conditions and the mathematically intractable form of the problem.

EXPERIMENTATION

A study was undertaken in which the effectiveness of various wind barrier configurations was evaluated to determine a practical design which would reduce the wind effect in the test area and, at the same time, increase the operating time available for experiments in the simulated rain field.

Since studies by Jensen [3], Nägeli [4] and others [5-12] have shown as much as 70 to 80% reduction in wind speed on the lee side of dense barriers, with correspondingly smaller reductions behind less dense barriers, it was believed that a practical, effective wind barrier could be designed for the sled track rain field. Both wind tunnel and field studies were undertaken to determine the barrier configuration desired and to estimate the probable magnitude of wind speed reduction.

Wind Tunnel Barrier Experiments

Barriers 15 cm high (scale 1:40) and extending the width of the wind tunnel were placed in the test section, and wind speed measurements were taken at various locations behind the barrier using a hot-film anemometer probe. Tests were run to determine the effects of (a) barrier permeability, (b) ambient wind speed, and (c) a flap affixed to the top of the barrier. Wind tunnel instrumentation and simulation are discussed in Appendix A.

Changing the ambient wind speed between 5 and 15 m/sec appeared to have little effect on the normalized wind values, so all subsequent tests were run at an ambient speed of about 5 m/s.

Three barriers having hole areas of 0, 35, and 60% were used to determine the effect of hole area on barrier effectiveness. Measurements were made at distances equal to 1 to 6 bh behind the barrier at a height of .5 bh for the 0 and 35% barriers, and at .25 bh for the 60% barriers. The results are shown in Figure 3. The 60%-hole-area barrier is quite ineffective at all distances behind the barrier, even at .25 bh above the floor. The solid barrier is best to a distance equal to 1.5 bh downstream but is much less efficient than the 35%-hole-area barrier at greater distances. Since the region of interest is 2 to 4 bh behind the barrier, it appeared that a 35%-hole-area barrier was most promising.

More information about the wind field behind the 35%-hole-area barrier was desired. Wind speed measurements were made at heights of .25, .5, .75, 1, 1.25, and 1.5 bh at 1, 2, 3, 4, 5, and 6 bh behind the barrier. The normalized wind (measured flow velocity divided by mean tunnel wind velocity) speeds are shown in Table 1. These values were used to plot isotachs as shown in Figure 4. At distances equal to 3 to 4 bh to the lee of the barrier, wind speed reductions of 80% or more are realized to heights of approximately one bh.

A sheet metal flap 5 cm wide and the same length as the barrier was affixed horizontally to the top of the barrier extending leeward in an attempt to reduce turbulence behind the barrier. Little difference

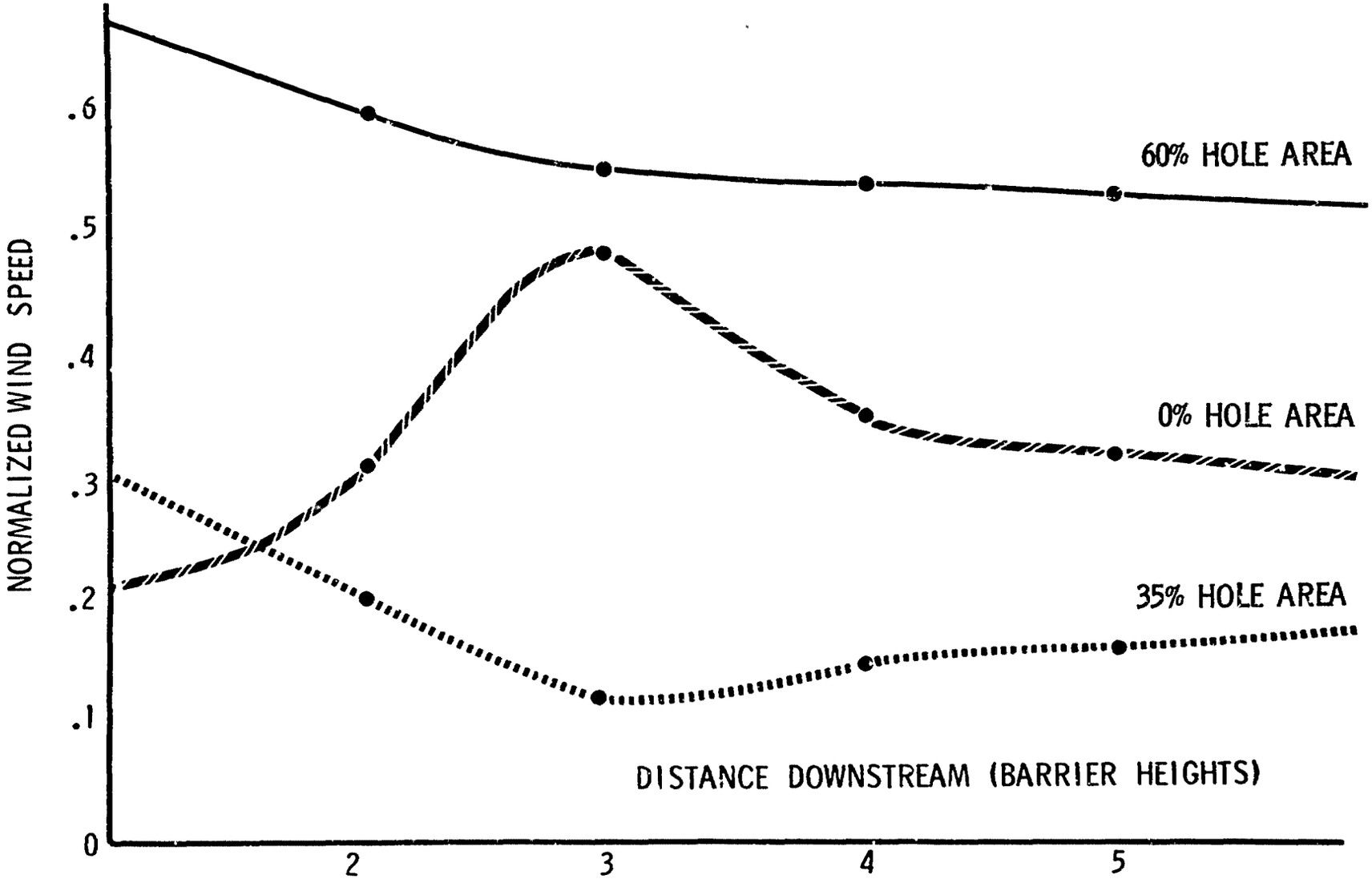

Figure 3. Wind tunnel comparison of barrier effectiveness.

TABLE I

NORMALIZED WIND SPEEDS FROM WIND TUNNEL TESTS U/U_o

AMBIENT FREE FLOW IN TUNNEL = $U_o = 3.5 \pm 0.06$ m/s

Vertical Position of Sensor (bh)	NORMALIZED WIND SPEEDS						
	0	1	2	3	4	5	6
1.50	1.10	0.67	0.54	0.49	0.46	0.44	
1.25	0.42	0.40	0.27	0.27	0.27	0.30	
1.00	0.39	0.30	0.21	0.20	0.19	0.21	
.75	0.35	0.19	0.17	0.17	0.20	0.18	
.50	0.27	0.16	0.15	0.16	0.17	0.16	
.25	0.16	0.12	0.12	0.13	0.15	0.15	

Distance Downstream from Barrier (in terms of barrier height)

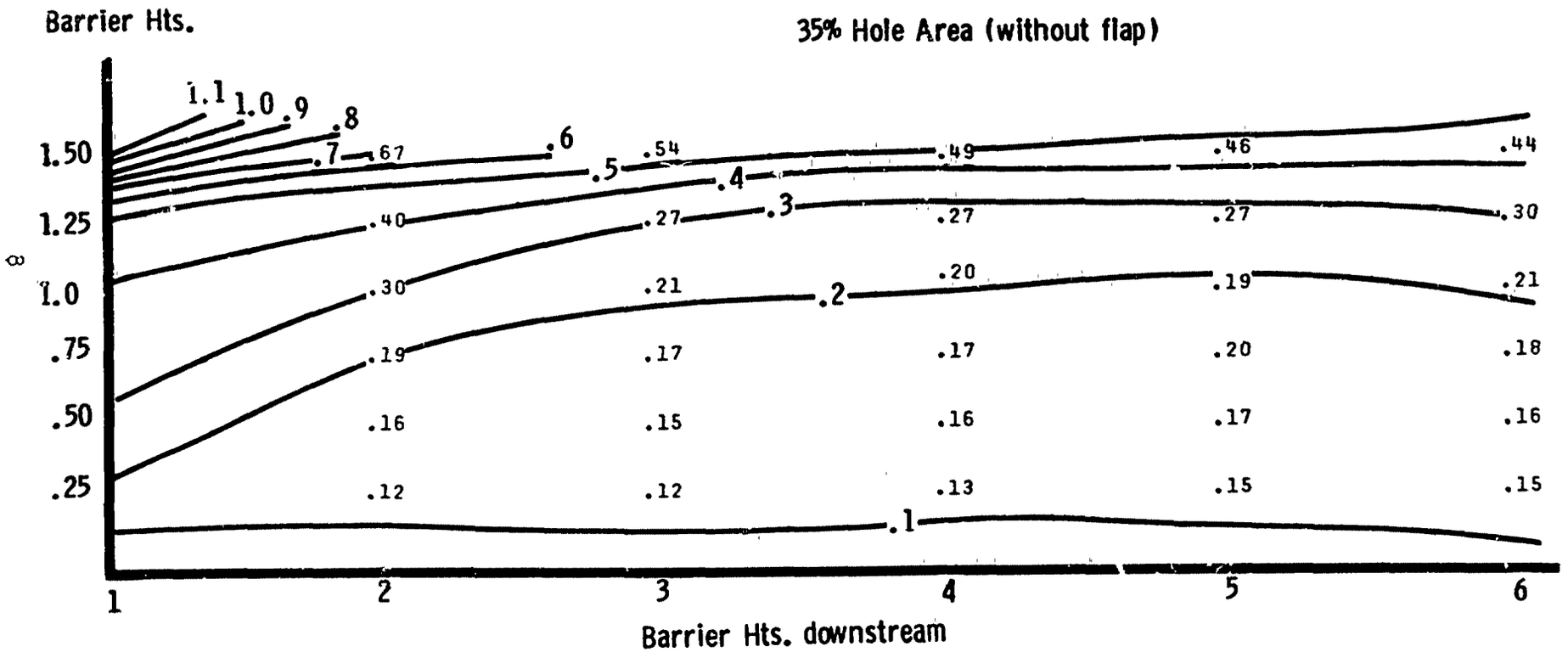

Figure 4. Downstream isotach field, wind tunnel test.

was observed between wind speed profiles when the flap was used and when it was not, although the flap did produce slightly more laminar flow and slightly lighter wind speeds close to the floor.

Field Tests

To check the validity of the wind tunnel data and to provide a means to scale up to the dimensions of the desired wind barrier, a field prototype barrier was constructed. It consisted of a chain link fence, 30 m long and 2.1 m high, with diagonal aluminum slats (Figure 5). The top .3 m of the fence was inclined at a 45° angle. The hole area was estimated to be 30 to 40%, about the same as the optimal hole area in wind tunnel experiments.

Wind measurements were made in front of and behind the fence with low-threshold cup anemometers (output was integrated to give mean wind speed) and a wind vane for wind direction measurements.

First Experiment

Initially, anemometers were set at 1/2 fence height at distances of 1.5, 3, and 6 fence heights to the lee of the fence and 6 fence heights to the windward side. Fifteen-minute averages of wind speed and direction were recorded. Visual evidence (Figures 8&9) show that for the porous barrier, variabilities about these averages for a steady wind are small. The wind speeds were normalized by dividing by the windward anemometer reading at the same height. Table II gives data for winds with large components perpendicular to the fence (normal $\pm$ 30°). Because the wind direction is extremely variable in light winds, the 15-minute average may include winds from directions quite different from the indicated mean.

Second Experiment

In a second experiment, conducted during a steady 3 to 5 m/sec wind, three anemometers were mounted on a mast at heights of .9, 1.8, and 2.7 m. A fourth anemometer was placed 18 m to the windward side of the fence at a height of .9 m to give average ambient wind. The mast was placed successively at 1.5, 3, and 6 m in front of and behind the fence and against the fence, and 5-minute averages were collected in each location. These were normalized by dividing by the wind speed obtained with the fourth anemometer. Results of the experiment are shown in Table III, and the isotachs are plotted in Figure 6.

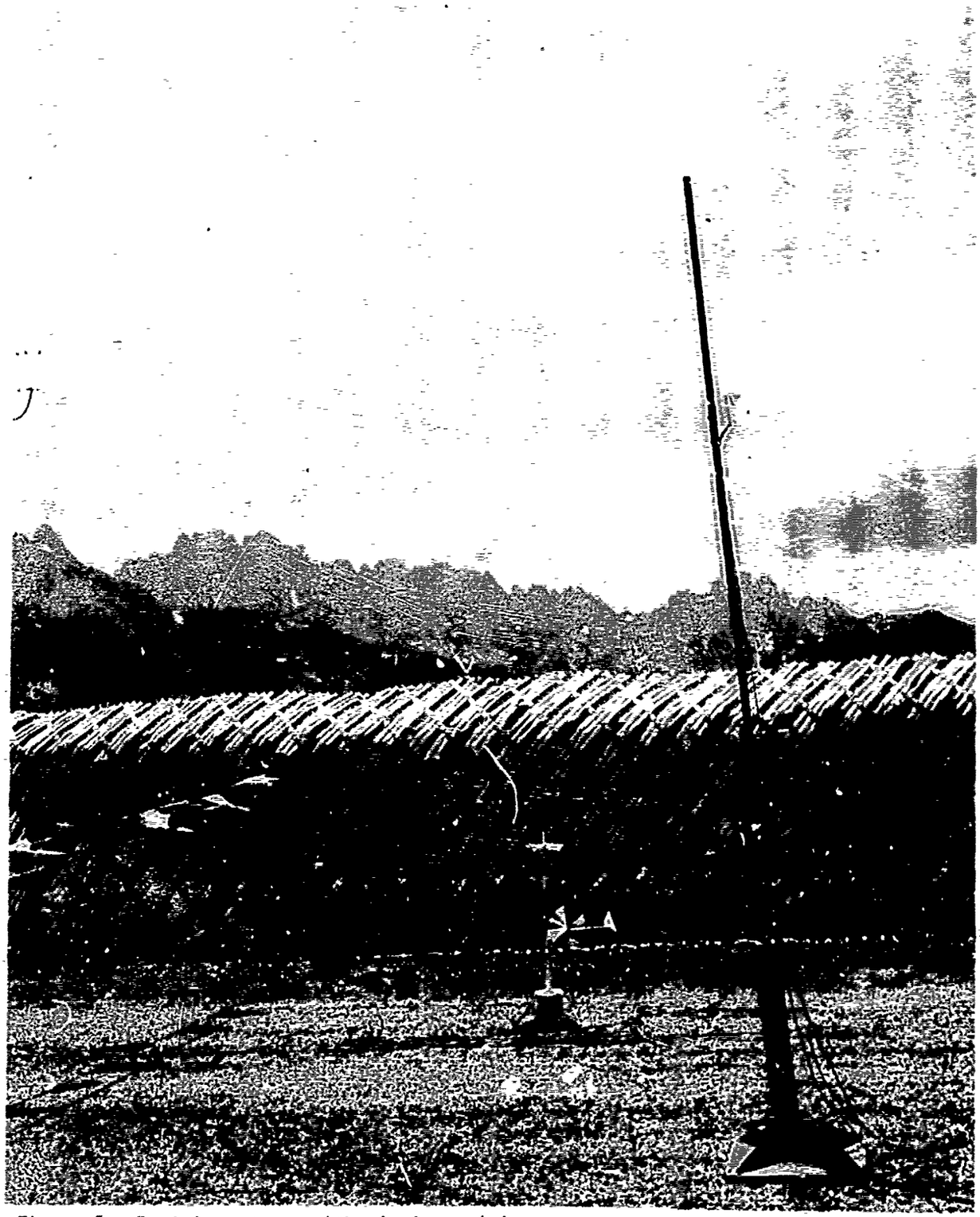

Figure 5. Prototype fence with aluminum slats.

TABLE II

THESE DATA ARE FOR WINDS PERPENDICULAR (WITHIN ± 30° OF NORMAL) TO THE PROTOTYPE BARRIER (OVER 15-MINUTE INTERVALS)

MEAN DIRECTION (DEGREES)	MEAN AMBIENT WIND SPEED (METERS/SECOND)	NORMALIZED WIND SPEEDS 1.5 bh DOWNSTREAM	3 bh DOWNSTREAM	6 bh DOWNSTREAM
294	0.80	0.01	0.15	0.55
286	1.24	0.18	0.42	0.68
288	1.13	0.01	0.12	0.35
251	1.24	0.06	0.23	0.56
269	1.21	0.02	0.13	0.42
285	0.83	0.29	0.54	0.75
271	1.15	0.00	0.03	0.31
281	1.08	0.23	0.40	0.59
281	0.55	0.02	0.44	0.84
248	1.27	0.01	0.13	0.39
290	0.85	0.00	0.07	0.48
270	1.24	0.00	0.09	0.40
279	1.54	0.10	0.19	0.42
251	1.95	0.19	0.28	0.54
260	2.36	0.19	0.28	0.51
249	2.79	0.20	0.29	0.51
255	2.74	0.19	0.27	0.50
286	2.45	0.22	0.30	0.59
293	2.15	0.20	0.23	0.43
287	2.92	0.26	0.29	0.52
286	1.35	0.08	0.14	0.36

Wind Sensor Vertical Position was 1/2 Barrier Height

TABLE III

AMBIENT WIND SPEED 3.6 ± 0.9 m/sec WIND DIRECTION--FROM THE EAST

Vertical Position of Sensors	6E	3E	1.5E	0.2E	1.5W	3W	6W	12W	
2.7 m	141	139	150	371	438	127	102	123	Pulses
	1.06	1.15	1.04	1.22	1.20	0.91	0.65	1.08	NWS*
1.8 m	130	125	128	297	92	32	41	88	Pulses
	0.98	1.03	0.89	0.98	0.26	0.23	0.26	0.77	NWS*
.9 m	113	106	100	153	111	45	34	65	Pulses
	0.85	0.88	0.69	0.50	0.31	0.82	0.22	0.57	NWS*
	HORIZONTAL POSITION OF SENSORS (M)								
Control	133	121	144	304	357	140	158	114	Pulses

Data taken as pulses and normalized by simultaneous measurements at control instrument in ambient flow.

Data taken 12 m west were influenced by 0.8 m ridge parallel to fence which would be expected to increase wind velocity measured at this station.

*NWS denotes Normalized Wind Speed = $\frac{\text{pulses}}{\text{control pulses}}$.

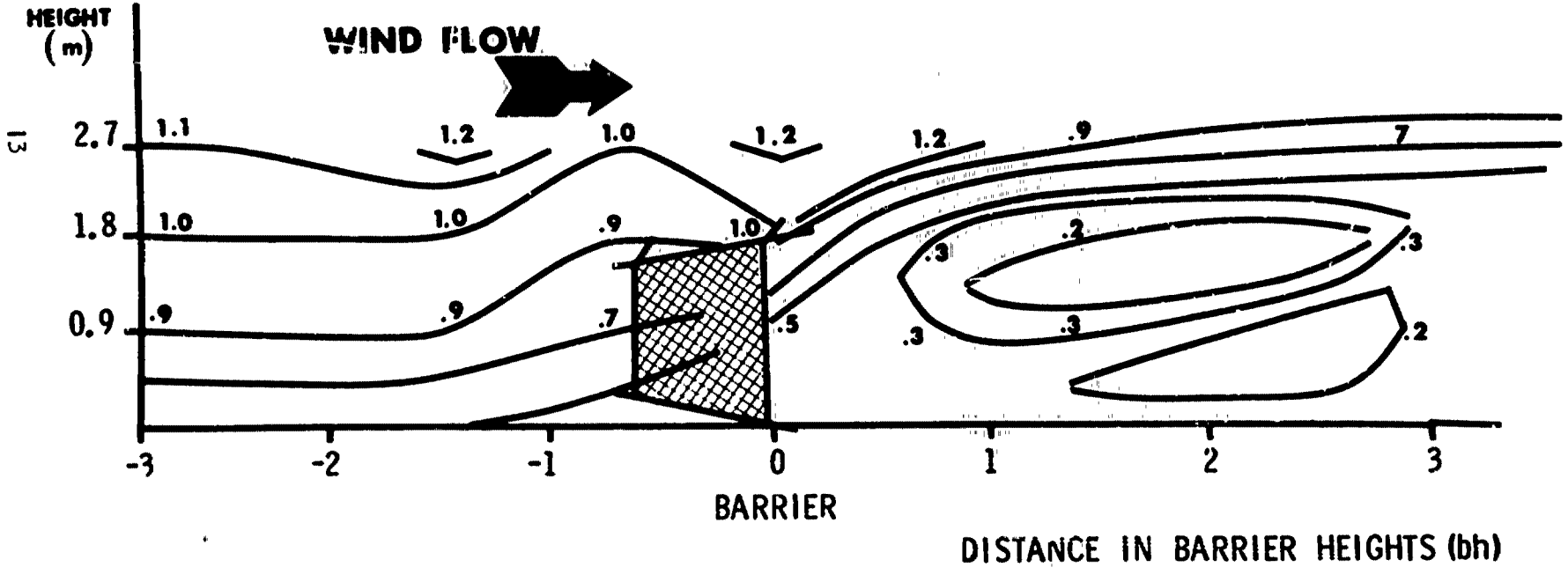

Figure 6. Isotachs of normalized wind speed, prototype barrier.

The isotach patterns of Figure 6 show relative velocity minimums below 0.2 U_o downstream of the fence, demonstrating the effectiveness of the prototype barrier in a form directly applicable to rain field tests at the rocket sled test track, decreasing the wind field, particularly cross-wind components, during simulation tests. In addition, it is evident from the normalized streamlines (Figure 7) that an upward component is induced in the flow approaching the barrier on the upstream side. This effect persists downstream of the barrier for at least 3 bh. One sees that the barrier acts in such a way as to transform a portion of the horizontal momentum of the flow to a vertical component. The streamline analysis in Figure 7 may also be compared with the smoke flow over and through the partially porous fence illustrated in Figure 8. Smoke grenades were released in the vicinity of the fence to provide qualitative information. In one case for .6-1.2 m/s easterly winds, the movement of the smoke over and through the fence was photographed. Just as the streamlines indicate speedup in the flow immediately above the fence, smoke pouring rapidly over the top of the fence is evident in the photograph. There is a definite tendency for the smoke to "pile up" in front of the fence and go over or filter through more slowly. Movies, taken from behind the fence, of the smoke passing through and over the fence showed smoke puffs reaching and going over the fence with little change in speed while some time was required for smoke to filter through the fence. The stagnant smoke behind the fence in Figure 9 may again be compared with the diverging streamlines downstream of the fence in Figure 7. Note that there is little smoke movement until the smoke reaches about fence height.

Comparison of Figures 4 and 6 and Geiger's Figure 1 [1] indicates that the wind tunnel barrier, the fence, and the dense shelter belt affect wind flow similarly. The smoke studies (Figures 8 and 9) show flow patterns similar to those given by the wind speed measurements. All of the studies indicate a 70 to 80% reduction in the wind component perpendicular to the fence.

The streamline analysis of Figure 6 indicates the decrease in downstream velocity and increase in vertical velocity component engendered by the barrier. Values of the average wind speed over a 1.8 m height range both upwind and downwind of the obstacle are shown in Figure 10. Figure 11 delineates the average wind defect under east and west wind conditions as a function of distance from the prototype barrier. Measurements at a height of .9 m were taken over a span of several days for these averaged data. (See Tables IV and V.) These long-term data may be compared with the shorter-term samples shown in Figure 6. Wind defects of 71% and 84% are indicated at distances of 1.5 bh downstream in Figure 11. These data were taken under conditions of generally light and variable winds at the site. The data in Figures 6 and 10 indicate that the barrier effect may be observed further downstream under conditions of stronger and steadier flow.

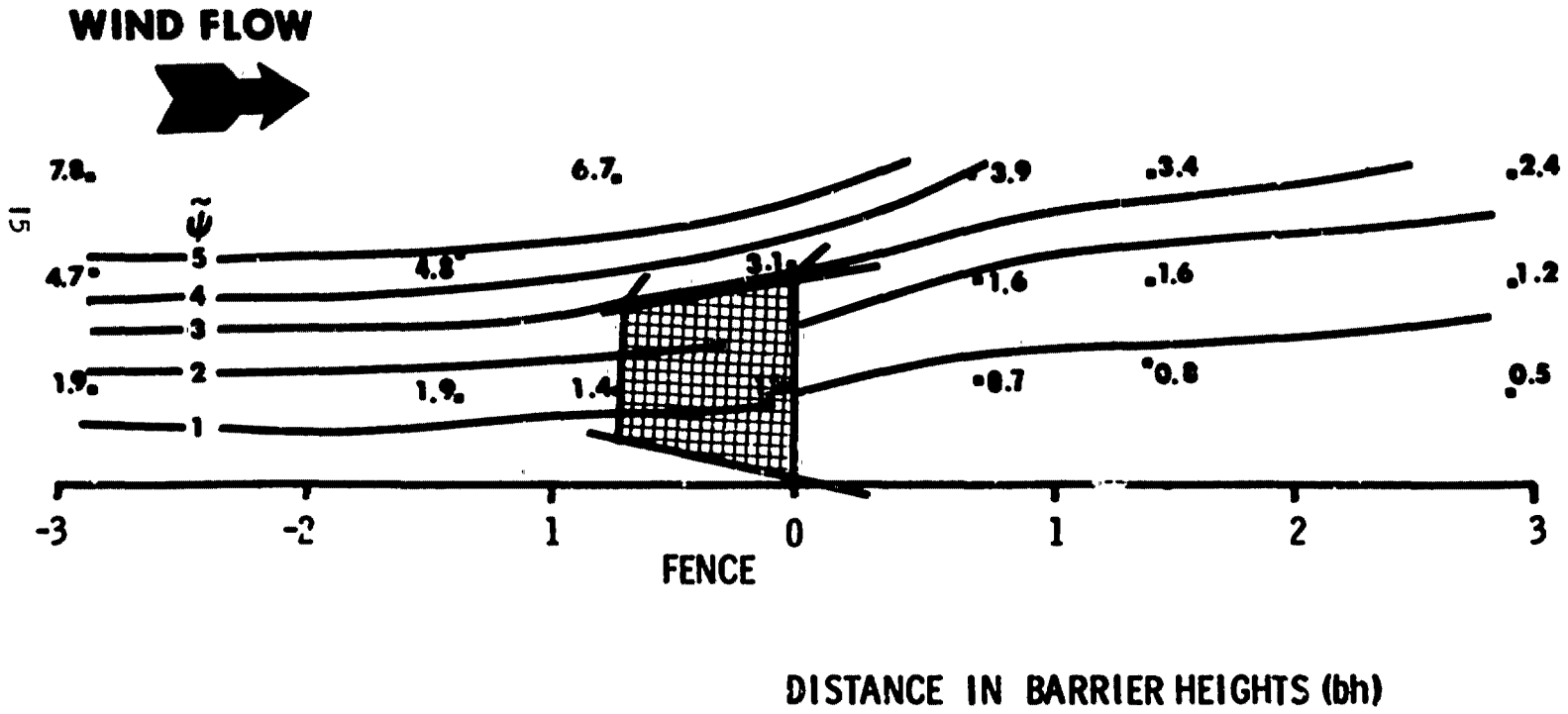

Figure 7. Streamline analysis, prototype barrier.

Figure 8. Smoke tracer release upstream of barrier.

Figure 9. Downstream smoke trailer release non-prototype barrier.

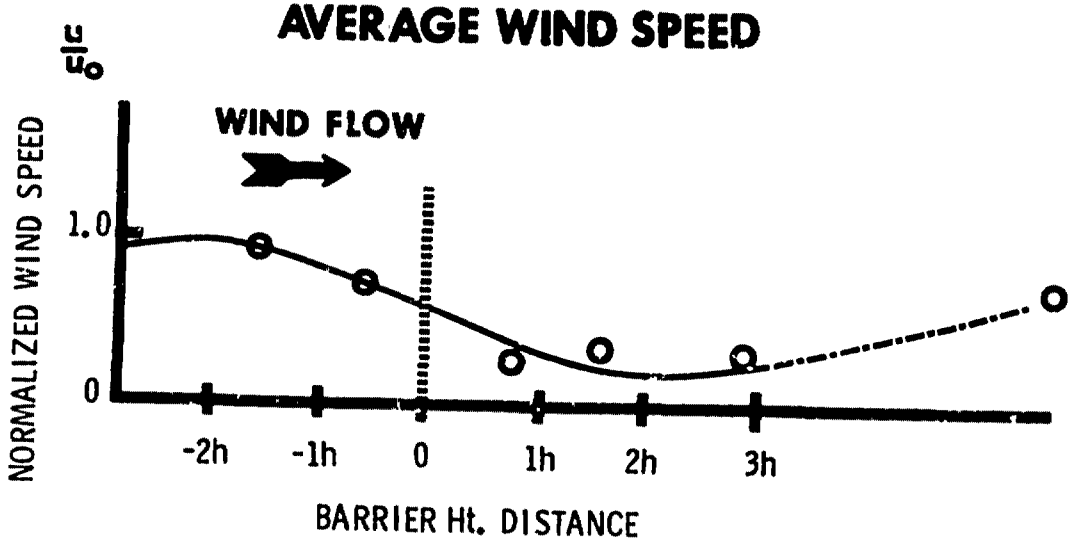

Figure 10. Mean wind speed, 0-2 m, prototype barrier.

TABLE IV

15-MINUTE AVERAGED WIND DATA

DATE (Aug 1970)	TIME (MDT)	WIND DIRECTION (DEGREES)	POSITION WITH RESPECT TO BARRIER (M) 6E	3E	3W	6W	12E	12W
04	0145	078	120/108	86/103	64/077	93/111		
03	1928	127	317/286	81/256	29/93	40/128		
03	1913	120	337/304	83/279	29/97	28/95		
03	1828	124	444/400	82/363	31/136	38/167		
03	1743	121	366/330	80/294	30/110	37/137		
03	1628	109	332/209	81/269	24/079	29/097		
03	1613	125	299/269	80/240	32/96	42/127		
03	1513	101	206/186	82/169	34/71	50/103		
03	1458	114	295/266	81/238	33/98	43/128		
03	1443	105	278/250	82/227	27/104	63/175		
03	1428	119	282/254	82/230	46/129	70/197		
03	1258	090	162/146	84/136			101/163	81/131
03	1313	114	222/200	80/178			96/213	71/157
03	1243	095	311/280	80/248			97/302	54/169
03	1228	098	151/136	81/123			100/151	79/119
03	1158	116	179/161	79/141			99/178	62/111
03	1113	096	173/156	82/141			92/159	88/153
03	1038	067	151/136	83/126			97/146	88/133
04	1315	112	430/387	78/341	27/115	28/122		
04	1300	112	493/444	80/395	27/135	33/162		
04	1230	119	503/453	81/409	28/141	34/173		
04	1215	115	373/336	82/304	29/109	40/150		
04	1200	092	230/207	82/188	27/61	32/73		
04	1145	112	240/216	79/190	25/61	38/90		
04	1045	115	159/143	79/126	23/37	37/59		
04	0945	112	134/121	78/104	28/38	44/59		
04	0930	110	117/105	81/95	32/37	59/69		
04	0915	116	114/103	80/91	22/25	55/63		
04	0900	111	143/129	80/114	29/29	42/60		
04	0845	080	246/222	78/193	6/39	19/46		
04	0830	06[illegible]	162/146	79/128	20/32	40/65		

In 6E column, numbers to right of slash are measured winds, cm/sec. Numbers to left of slash are computed Free Stream Flow velocities assuming the 6E data to be 90% of free stream flow, e.g., using the first entry, 108 X 10/9 = 120 cm/sec, the computed free stream flow. In columns 3E, 3W, 6W, 12E and 12W, the number to the right of the slash is measured speed; to the left the number is % of free stream flow, e.g., in column 6W 111 cm/sec is 93% of free stream flow (120 cm/sec).

TABLE V

15-MINUTE AVERAGED WIND DATA

DATE (AUG 1970)	TIME (MDT)	WIND DIRECTION (DEGREES)	POSITION WITH RESPECT TO BARRIER (M) 6E	3E	3W	6W*
04	0759	290	56/39†	24/17	87/61	70/63††
04	0659	269	33/30	10/09	74/67	91/82
04	0644	291	45/62	30/41	81/111	137/123
04	0629	306	45/63	26/31	76/91	119/102
04	0615	285	27/28	15/16	73/76	104/94
04	0545	293	34/23	05/03	64/43	67/60
04	0430	293	34/36	21/22	75/79	105/95
04	0400	286	30/24	08/06	73/58	80/72
04	0345	287	31/28	10/09	75/67	89/80
04	0330	282	32/30	07/07	75/71	95/86

*6W data are measured winds, cm/sec, assumed 90% of free stream flow (U_o)

†Format is % Free Stream/Measured Speed (cm/sec)

††Format is $\frac{10}{9}$ x Speed/Measured Speed

Example: At 6W measured speed = 63 cm/sec: calculated free stream flow, $U_o = \frac{10}{9} \times 63 = 70$ cm/sec. At 6E measured speed of 39 cm/sec is 56% of free stream flow.

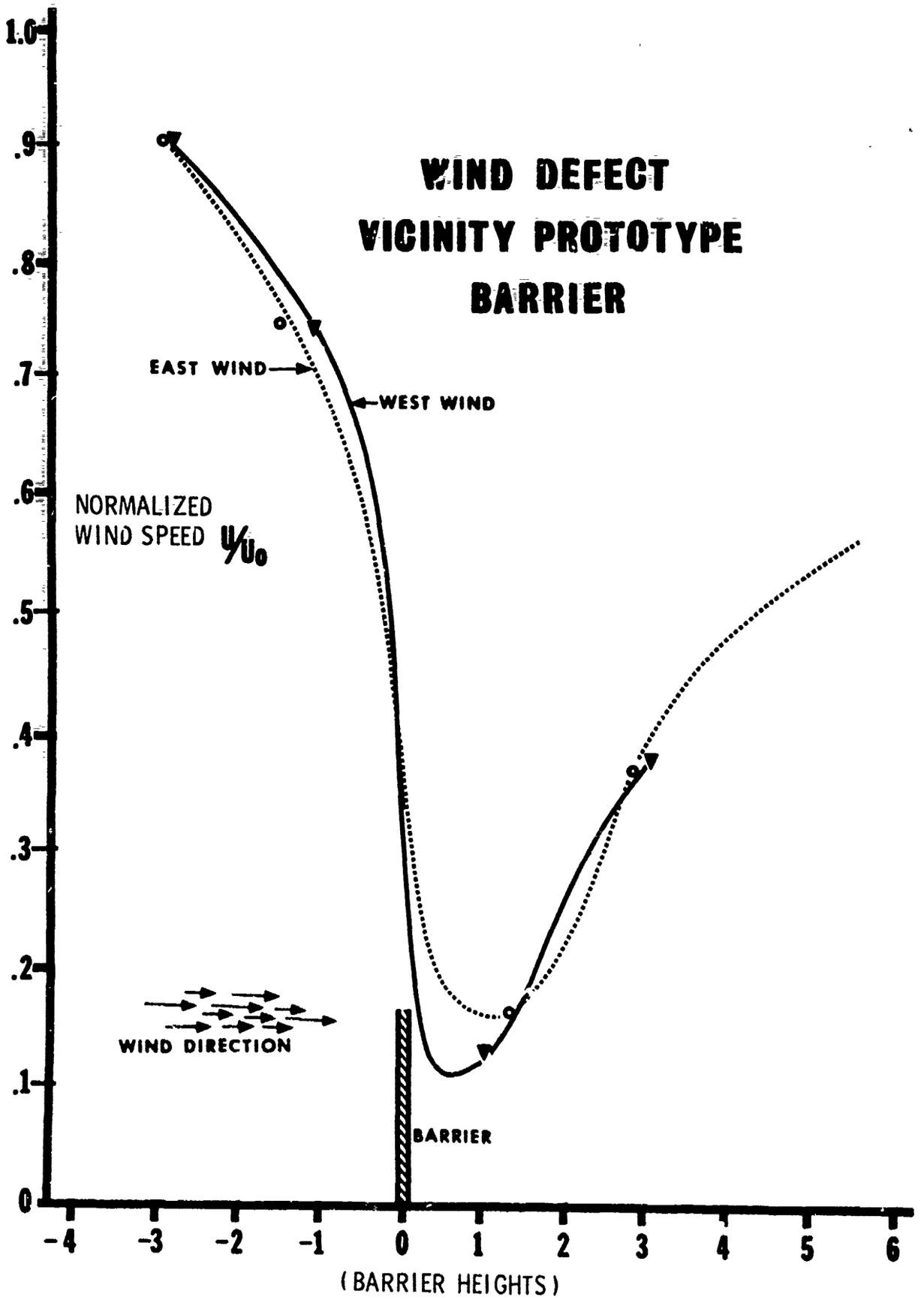

Figure 11. Mean wind defect, prototype barrier, for east winds and west winds. 21

Environmental Factors

To interpret the preceding in terms of the test track requirements, several salient environmental factors should be considered, including test track climatology, peak gust data, and terrain effects of the wind field in the test track area. Limited amounts of specific wind data from the rain field at the test track lead one to consider the climatology of nearby observing stations to be interpreted in terms of expected conditions at the test track itself. WSMR meteorological records relating to strong winds [13] (Table VI) show an all-time peak gust of 82 knots from the southwest. Maximum monthly mean winds for the year may be expected during March and April from a westerly direction.

While the paucity of wind data from the test track area per se poses a handicap, one would nonetheless recommend that a wind barrier configuration of maximum efficiency in decreasing cross-wind effects be designed. An idea of the expected percent increase in time available for testing is shown in Table VI', excerpted from 20-year Holloman AFB wind records. One should also mention that, in addition to increasing available test time, the barrier concept will also provide more hours of lower mean cross-wind velocities, thereby enhancing test control conditions.

One important local effect on the winds across the test track comes from the venturi created by an arroyo located to the west of the center of the rain field. The channeling or venturi effect under westerly flow conditions could cause significantly higher mean winds and peak gusts in the area at times.

SUMMARY AND CONCLUSIONS

Studies undertaken show that the critical factors in wind barrier protection are barrier height and permeability. The barrier height is primarily important in determining the extent of wind defect one may achieve, while barrier permeability is critical in determining the region over which the wind defect is near or at its maximum. Moreover, permeable fences widen the region of large wind defect, making for much greater reliability in scaling from a prototype test barrier to actual barrier specifications recommended for the Holloman facility.

Agreement between wind tunnel results and field tests with the 2 m prototype fence was consistent. Similar wind defects at corresponding downstream distances were found in the two cases. In addition, visual evidence supplied by photographs and motion pictures supported the measured wind data.

TABLE VI

MAXIMUM WINDS (STRONGEST GUSTS IN KNOTS), 1950-1961

"A" STATION, WHITE SANDS MISSILE RANGE

YEAR	JAN.	FEB.	MAR.	APR.	MAY	JUNE	JULY	AUG.	SEP.	OCT.	NOV.	DEC.
1950	31SW	27NE	35SW	26WSW	35W	26W	26NW	22W	22SSE	17SE	35W	30W
1951	56SW	65WSW	74W	56SW	48W	45SSW	43SSE	45S	35S	43WNW	56W	82SW
1952	56W	27NNW	26NW	31W	27S	25SSE	30SSW	43NNW	22W	17SE	48W	49S
1953	56NW	68SW	54SW	56W	55SW	- - -	37NW	26NW	26SSW	22SE	43NW	65N
1954	35W	62WNW	65W	40WNW	48W	21W	44E	40NE	32SSE	45W	53W	47WNW
1955	46WNW	40W	64W	66W	48W	49W	36N	32SE	32S	35W	56W	46WSW
1956	64S	64WNW	56W	60W	64W	42W	36SW	32SSW	35SSE	46WSW	47WNW	52W
1957	65WSW	40NW	54WNW	66WSW	59WSW	53WNW	33S	51SSE	37NNW	52WNW	38WSW	50WSW
1958	51WSW	63SW	60W	66WSW	43W	37W	36WSW	33NW	30NE	26WNW	45SW	46WSW
1959	70W	56W	52W	44W	43W	40N	34ENE	30S	39ESE	41SW	45WSW	70W
1960	57WNW	63WNW	45W	52W	40W	34S	32E	28S	35WSW	41W	54W	56W
1961	35W	52W	64WSW	49W	74WSW	40W	34SSE	27SSE	40W	60SW	56WNW	56S
XTRMS:	70W	68SW*	74W	64W*	74SSW	53WNW	44E	51SSE	40W	60SW	56W*	82SW

*MORE THAN ONE OCCURRENCE.

TABLE VII

WIND CLIMATOLOGY, HOLLOMAN AFB, NM, ALL HOURS AND ALL WEATHER
WITH MODIFICATIONS EXPECTED FROM A 70% WIND DEFECT

	PERCENT OF TIME WIND ≤ 3kt	PERCENT OF TIME WIND ≤ 10kt WITH 70% DEFECT ≤ 3kt	% INCREASE IN TIME
JAN	41.5	89.5	107
FEB	35.8	86.8	142
MAR	30.4	81.4	168
APR	27.4	80.2	189
MAY	26.8	80.7	201
JUNE	29.3	83.4	185
JULY	32.2	88.6	175
AUG	35.9	91.1	154
SEP	39.2	91.5	133
OCT	46.2	93.2	102
NOV	45.3	91.3	101
DEC	41.5	91.4	108

RECOMMENDATIONS

The area of the test track in need of wind protection extends 3-4 m above the ambient ground level at the rails. The empirical results obtained in the wind tunnel and from prototype investigations indicate a wind speed minimum at a scale distance of 2 to 3 bh downstream from the barrier for free-stream speeds in the 2-5 m/sec range. No appreciable effect from air circulating around the end of the barrier was apparent at stations located near the center of the prototype barrier. The recommended extension, therefore, on each end of the barrier protection zones is a minimum of 15 m and a maximum of 30 m for wind velocities within $\pm 30°$ of flow normal to the barrier. For sufficient protection of the critical rain field test area the proposed barrier configuration is:

Height	6 m
Upstream Distance	15 m
Hole Area	35%

One would recommend that the barrier be built to conform to the arroyo or that a large land fill be designed to allow for consistent barrier protection over the entire length of the rain field. If the decision were made to follow the terrain with the fence, the hole area of the fence should decrease closer to the test track, as indicated by the wind tunnel results of Figure 3. In addition, since the rain field is known to be affected significantly by light winds, a dual wind barrier with one segment on each side of the track may well be desirable.

APPENDIX A

Wind Tunnel

Wind tunnel simulation measurements were made in the ASL low-speed wind tunnel facility at WSMR. The wind tunnel employed is a closed-circuit system (Figure 12) in which air moves from a propeller section through a round-to-square transition section and then through a gradually increasing square section to a first corner. The square corners are constructed with turning vanes which direct the air to a second square corner and into a contraction section. At the head of the contraction section is a set of four fine mesh screens for turbulence reduction. The contraction section follows an exponential function in design and has a contraction ratio of 5:1.

From the contraction section the air flows through a 1.2 by 1.2 by 2 meter test section in which the barrier experiments were conducted. The test section is isolated from the main structure by foam rubber inserts to reduce vibration. The air then moves through an expansion section, a square-to-round transition, two sets of turning vanes, and then returns to the propeller section. Maximum propeller speed is 840 rpm. The turning vanes are designed for the low-speed flow generated in this wind tunnel [14].

Since the facility is a low turbulence wind tunnel, the simulation data represent the most precise measurements of barrier flow phenomena available. Possible minor error sources exist arising from finite fence width across the tunnel floor and residual turbulence effects in the tunnel in addition to the normal errors occasioned by the recording of the experimental data [15].

Reynolds number calculations for the wind tunnel model, fence, and prototype lie within an order of magnitude for cases a, c, and e, as listed in Table VIII. Thus it becomes reasonable to apply the results from the wind tunnel simulation data and the prototype fence data to design recommendations for the rain field barrier at the rocket sled test track. Reasonable results in terms of Reynolds number modeling for flow around sharp-edged obstacles may be obtained by geometric simulation alone as indicated by Chein [16], Goldstein [17], and Cermak and Horn [18]. The fence barriers are sufficiently angular so that the flow patterns around them (Figure 13) are largely independent of viscous influences and thus dynamic similarity may be achieved at lower wind tunnel speeds than would otherwise be possible. The results of Figure 13 were obtained from flow visualization tests conducted in the University of Notre Dame low turbulence subsonic wind tunnel.

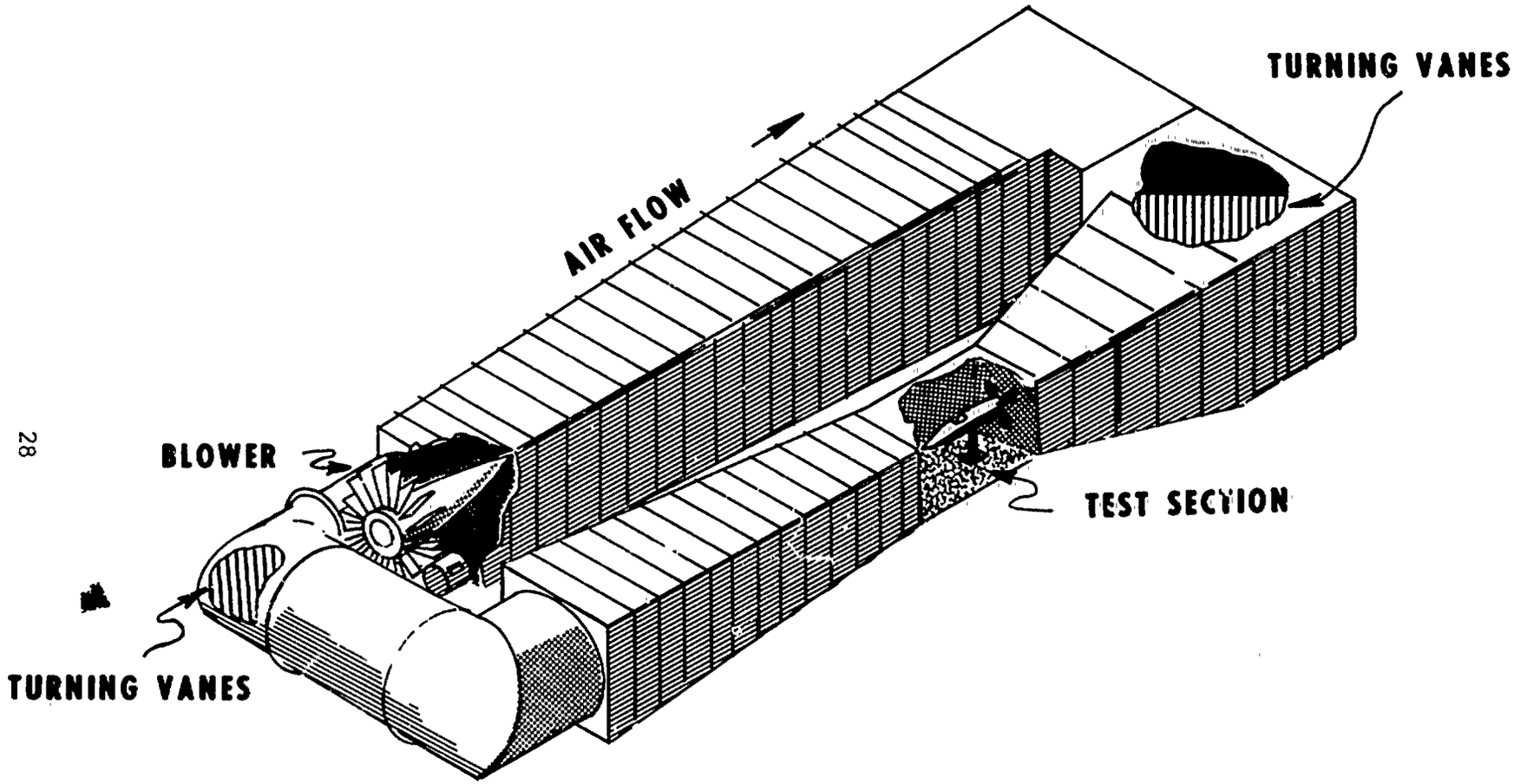

Figure 12. ASL wind tunnel, cutaway sketch.

TABLE VIII

DETERMINATION OF REYNOLDS NUMBER FOR SIMILARITY ANALYSIS OF MODEL AND PROTOTYPE BARRIERS

CASE	MODEL DIMENSION	VELOCITY (m/sec)	$Re = \frac{U\ell}{\nu}$
a	15 cm model in tunnel	15	1.1×10^5
b	15 cm model in tunnel	5	0.4×10^5
c	2 m slat fence	2	2.0×10^5
d	6 m barrier	5	15.0×10^5
e	6 m barrier	1	3.0×10^5

Kinematic viscosity, ν, is taken as 0.2 $cm^2 sec^{-1}$.

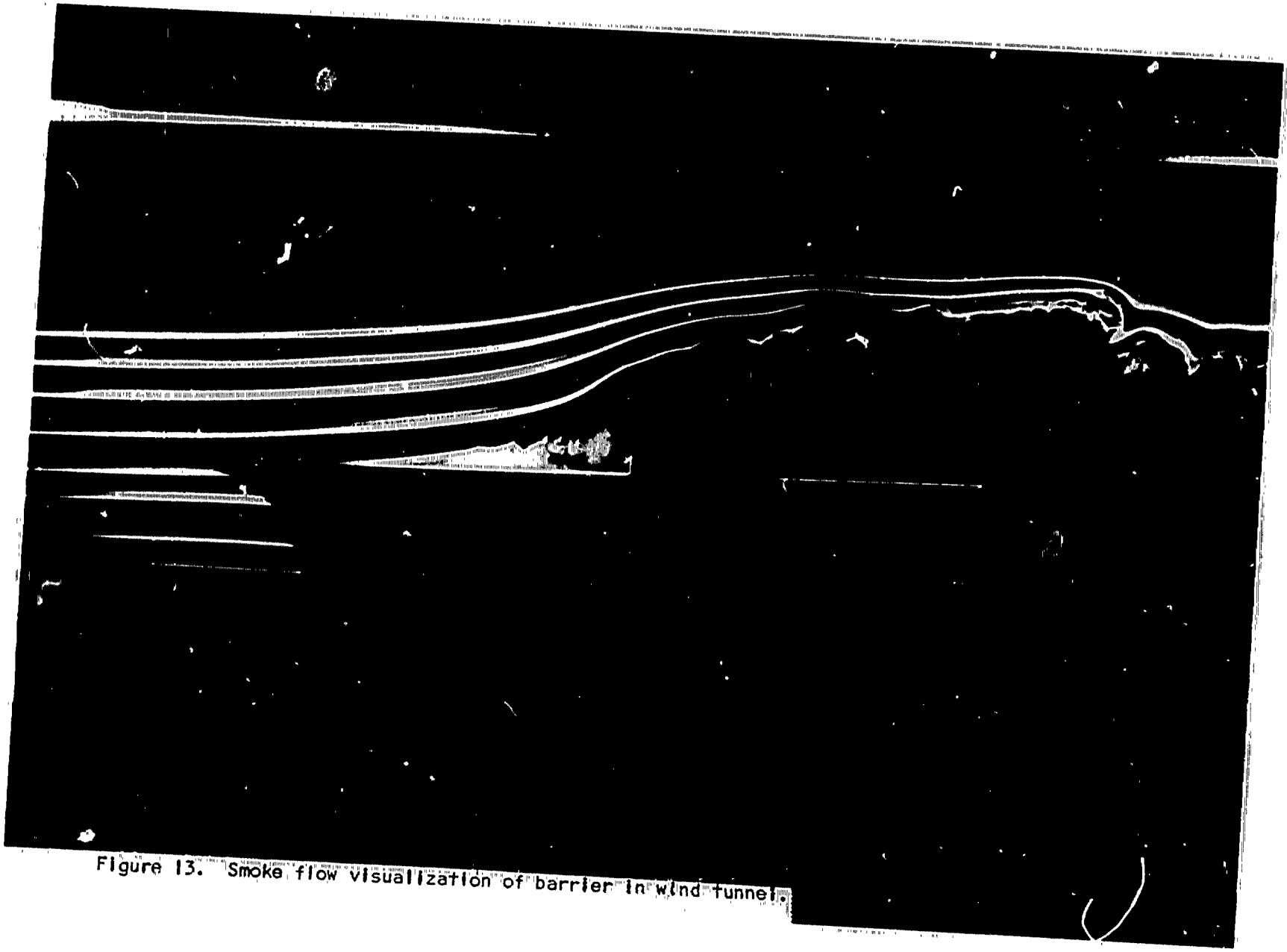

Figure 13. Smoke flow visualization of barrier in wind tunnel.

The wind tunnel flow measurement device used as a control in the test section is a propeller-anemometer (MRI Velocity Vane) mounted on the ceiling of the tunnel facing into the airstream. Velocity measurements for the barrier simulation tests were obtained with a TSI 1054B, hot-film constant-temperature anemometer. Turbulent scintillations were obtained from a Tektronix 564 oscilloscope and a B&K VTVM analyzer. Wind velocity defect data downstream of the barrier were read on a Fluke 805B potentiometer and recorded by an observer. Velocity data were obtained at stations located 1bh to 9bh downstream of the barrier at 1 bh intervals and from 0.25 to 1.5 bh above the tunnel floor.

LITERATURE CITED

1. Geiger, R., 1965, The Climate Near the Ground, Harvard University Press, Cambridge.

2. Sutton, O. G., 1949, Atmospheric Turbulence, London.

3. Jensen, Martin, 1961, Shelter Effect, Danish Technical Press, Copenhagen.

4. Nägeli, W., 1953, "Untersuchungen uber die Windverhaltnisse im Bereich von Schilfrohrwanden," Ebenda 29, 213-266.

5. Nägeli, W., 1946, "Untersuchungen uber die Windverhaltnisse im Bereich von Windschutzstreifen," Mitt. d. Schweiz. Anst. f. d. forstl. Versuchswesen 23, 221-276, 1943 and 24, 657-737.

6. Lindsay, R. B., 1960, Mechanical Radiation, McGraw-Hill Book Co., Inc., New York.

7. Mellor, Malcolm, 1965, "Cold Regions Science and Engineering, Part III Sect. A3c, Blowing Snow," U.S. Army Materiel Command, CRREL, Hanover, New Hampshire.

8. O'Hare, Michael, and Richard E. Kronauer, 1969, "Fence Designs to Keep Wind From Being a Nuisance," Architectural Record.

9. Plate, E. J., and C. W. Lin, 1965, "The Velocity Field Downstream from a Two-Dimensional Model Hill," Fluid Dynamics and Diffusion Laboratory, Colorado State University.

10. Schultz, H. L., and C. F. Kelly, 1960, "Studies on Wind Protection Efficiency of Slatted Fence Windbreakers," California Agriculture.

11. Trebble, W. J. C., 1960, "Wind-Tunnel Investigation of Airflow Past Blast Fences," Tech Note Aero 2728, Royal Aircraft Establishment, London.

12. Woodruff, N. P., R. A. Read, and W. S. Chepil, 1959, "Influence of a Field Windbreak on Summer Wind Movement and Air Temperature," TB100, Agricultural Experiment Station, Kansas State University.

13. Hoidale, M. M., B. J. Gee, and G. W. Harmon, 1968, "Atmospheric Structure, White Sands Missile Range, New Mexico, Part I, Surface Wind, Cloud Cover, Visibility," ECOM-5202, Atmospheric Sciences Laboratory, U.S. Army Electronics Command, White Sands Missile Range, New Mexico.

14. Pope, A., and J. J. Harper, 1966, Low-Speed Wind Tunnel Testing, John Wiley and Sons, New York.

15. Horn, J. D., 1967, "Simulation Studies of Wind Defects on Atmospheric Probes," Dept. of Physics, University of Texas at El Paso.

16. Chien, N., Y. Fong, H. Wang, and T. Siao, 1951, "Wind Tunnel Studies of Pressure Distribution of Elementary Building Forces," Iowa Institute of Hydraulic Research, State University of Iowa, Iowa City, Iowa.

17. Goldstein, S., 1938, Modern Developments in Fluid Dynamics, Oxford University Press.

18. Cermak, J. E., and J. D. Horn, 1968, "Tower Shadow Effect," J. Geo. Res., 73, pp 1869-1876.

ATMOSPHERIC SCIENCES RESEARCH PAPERS

1. Miers, B. T., and J. E. Morris, Mesospheric Winds Over Ascension Island in January, July 1970, ECOM-5312, AD 711851.
2. Webb, W. L., Electrical Structure of the D- and E-Region, July 1970, ECOM-5313, AD 714365.
3. Campbell, G. S., F. V. Hansen and R. A. Dise, Turbulence Data Derived from Measurements on the 32-Meter Tower Facility, White Sands Missile Range, New Mexico, July 1970, ECOM-5314, AD 711852.
4. Pries, T. H., Strong Surface Wind Gusts at Holloman AFB (March-May), July 1970, ECOM-5315, AD 711853.
5. D'Arcy, E. M., and B. F. Engebos, Wind Effects on Unguided Rockets Fired Near Maximum Range, July 1970, ECOM-5317, AD 711854.
6. Matonis, K., Evaluation of Tower Antenna Pedestal for Weather Radar Set AN/TPS-41, July 1970, ECOM-3317, AD 711520.
7. Monahan, H. H., and M. Armendariz, Gust Factor Variations with Height and Atmospheric Stability, August 1970, ECOM-5320, AD 711855.
8. Stenmark, E. B., and L. D. Drury, Micrometeorological Field Data from Davis, California; 1966-67 Runs Under Non-Advection Conditions, August 1970, ECOM-6051, AD 726390.
9. Stenmark, E. B., and L. D. Drury, Micrometeorological Field Data from Davis, California; 1966-67 Runs Under Advection Conditions, August 1970, ECOM-6052, AD 724612.
10. Stenmark, E. B., and L. D. Drury, Micrometeorological Field Data from Davis, California; 1967 Cooperative Field Experiment Runs, August 1970, ECOM-6053, AD 724613.
11. Rider, L. J., and M. Armendariz, Nocturnal Maximum Winds in the Planetary Boundary Layer at WSMR, August 1970, ECOM-5321, AD 712325.
12. Hansen, F. V., A Technique for Determining Vertical Gradients of Wind and Temperature for the Surface Boundary Layer, August 1970, ECOM-5324, AD 714366.
13. Hansen, F. V., An Examination of the Exponential Power Law in the Surface Boundary Layer, September 1970, ECOM-5326, AD 715349.
14. Miller, W. B., A. J. Blanco and L. E. Traylor, Impact Deflection Estimaters from Single Wind Measurements, September 1970, ECOM-5328, AD 716993.
15. Duncan, L. D., and R. K. Walters, Editing Radiosonde Angular Data, September 1970, ECOM-5330, AD 715351.
16. Duncan, L. D., and W. J. Vechione, Vacuum Tube Launchers and Boosters, September 1970, ECOM-5331, AD 715350.
17. Stenmark, E. B., A Computer Method for Retrieving Information on Articles, Reports and Presentations, September 1970, ECOM-6050, AD 724611.
18. Hudlow, M., Weather Radar Investigation on the BOMEX, September 1970, ECOM-3329, AD 714191.
19. Combs, A., Analysis of Low-Level Winds Over Vietnam, September 1970, ECOM-3346, AD 876935.
20. Rinehart, G. S., Humidity Generating Apperatus and Microscope Chamber for Use with Flowing Gas Atmospheres, October 1970, ECOM-5332, AD 716994.
21. Miers, B. T., R. O. Olsen, and E. P. Avara, Short Time Period Atmospheric Density Variations and a Determination of Density Errors from Selected Rocketsonde Sensors, October 1970, ECOM-5335.
22. Rinehart, G. S., Sulfates and Other Water Solubles Larger than 0.15μ Radius in a Continental Nonurban Atmosphere, October 1970, ECOM-5336, AD 716999.
23. Lindberg, J. D., The Uncertainty Principle: A Limitation on Meteor Trail Radar Wind Measurements, October 1970, ECOM-5337, AD 716996.
24. Randhawa, J. S., Technical Data Package for Rocket-Borne Ozone-Temperature Sensor, October 1970, ECOM-5338, AD 716997.

25. Devine, J. C., The Fort Huachuca Climate Calendar, October 1970, ECOM-6054.
26. Allen, J. T., Meteorological Support to US Army RDT&E Activities, Fiscal Year 1970 Annual Report, November 1970, ECOM-6055.
27. Shinn, J. H., An Introduction to the Hyperbolic Diffusion Equation, November 1970, ECOM-5341, AD 718616.
28. Avara, E. P., and M. Kays., Some Aspects of the Harmonic Analysis of Irregularly Spaced Data, November 1970, ECOM-5344, AD 720198.
29. Fabrici, J., Inv. of Isotopic Emitter for Nuclear Barometer, November 1970, ECOM-3349, AD 876461.
30. Levine, J. R., Summer Mesoscale Wind Study in the Republic of Vietnam, December 1970, ECOM-3375, AD 721585.
31. Petriw, A., Directional Ion Anemometer, December 1970, ECOM-3379, AD 720573.
32. Randhawa, J. S., B. H. Williams, and M. D. Kays, Meteorological Influence of a Solar Eclipse on the Stratosphere, December 1970, ECOM-5345, AD 720199.
33. Nordquist, Walter S., Jr., and N. L. Johnson, One-Dimensional Quasi-Time-Dependent Numerical Model of Cumulus Cloud Activity, December 1970, ECOM-5350, AD 722216.
34. Avara, E. P., The Analysis of Variance of Time Series Data Part I: One-Way Layout, January 1971, ECOM-5352, AD 721594.
35. Avara, E. P., The Analysis of Variance of Time Series Data Part II: Two-Way Layout, January 1971, ECOM-5353.
36. Avara, E. P., and M. Kays., The Effect of Interpolation of Data Upon the Harmonic Coefficients, January 1971, ECOM-5354, AD 721593.
37. Randhawa, J. S., Stratopause Diurnal Ozone Variation, January 1971, ECOM-5355, AD 721309.
38. Low, R. D. H., A Comprehensive Report on Nineteen Condensation Nuclei (Part II), January 1971, ECOM-5358.
39. Armendariz, M., L. J. Rider, G. Campbell, D. Favier and J. Serna, Turbulence Measurements from a T-Array of Sensors, February 1971, ECOM-5362, AD 726390.
40. Maynard, H., A Radix-2 Fourier Transform Program, February 1971, ECOM-5363, AD 726389.
41. Devine, J. C., Snowfalls at Fort Huachuca, Arizona, February 1971, ECOM-6056.
42. Devine, J. C., The Fort Huachuca, Arizona 15 Year Base Climate Calendar (1956-1970), February 1971, ECOM-6057.
43. Levine, J. R., Reduced Ceilings and Visibilities in Korea and Southeast Asia, March 1971, ECOM-3403, AD 722735.
44. Gerber, H., et al., Some Size Distribution Measurements of AgI Nuclei with an Aerosol Spectrometer, March 1971, ECOM-3414, AD 729331.
45. Engebos, B. F., and L. J. Rider, Vertical Wind Effects on the 2.75-inch Rocket, March 1971, ECOM-5365, AD 726321.
46. Rinehart, G. S., Evidence for Sulfate as a Major Condensation Nucleus Constituent in Nonurban Fog, March 1971, ECOM-5366.
47. Kennedy, B. W., E. P. Avara, and B. T. Miers, Data Reduction Program for Rocketsonde Temperatures, March 1971, ECOM-5367.
48. Hatch, W. H., A Study of Cloud Dynamics Utilizing Stereoscopic Photogrammetry, March 1971, ECOM-5368.
49. Williamson, L. E., Project Gun Probe Captive Impact Test Range, March 1971, ECOM-5369.
50. Henley, D. C., and G. B. Hoidale, Attenuation and Dispersion of Acoustic Energy by Atmospheric Dust, March 1971, ECOM-5370, AD 728103.
51. Cionco, R. M., Application of the Ideal Canopy Flow Concept to Natural and Artificial Roughness Elements, April 1971, ECOM-5372, AD 730638.
52. Randhawa, J. S., The Vertical Distribution of Ozone Near the Equator, April 1971, ECOM-5373.
53. Ethridge, G. A., A Method for Evaluating Model Parameters by Numerical Inversion, April 1971, ECOM-5374.

54. Collett, E., Stokes Parameters for Quantum Systems, April 1971, ECOM-3415, AD 729347.

55. Shinn, J. H., Steady-State Two-Dimensional Air Flow in Forests and the Disturbance of Surface Layer Flow by a Forest Wall, May 1971, ECOM-5383, AD 730681.

56. Miller, W. B., On Approximation of Mean and Variance-Covariance Matrices of Transformations of Joint Random Variables, May 1971, ECOM-5384, AD 730302.

57. Duncan, L. D., A Statistical Model for Estimation of Variability Variances from Noisy Data, May 1971, ECOM-5385.

58. Pries, T. H., and G. S. Campbell, Spectral Analyses of High-Frequency Atmospheric Temperature Fluctuations, May 1971, ECOM-5387.

59. Miller, W. B., A. J. Blanco, and L. E. Traylor, A Least-Squares Weighted-Layer Technique for Prediction of Upper Wind Effects on Unguided Rockets, June 1971, ECOM-5388, AD 729792.

60. Rubio, R., J. Smith and D. Maxwell, A Capacitance Electron Density Probe, June 1971, ECOM-5390.

61. Duncan, L. D., Redundant Measurements in Atmospheric Variability Experiments, June 1971, ECOM-5391.

62. Engebos, B. F., Comparisons of Coordinate Systems and Transformations for Trajectory Simulations, July 1971, ECOM-5397.

63. Hudlow, M. D., Weather Radar Investigations on an Artillery Test Conducted in the Panama Canal Zone, July 1971, ECOM-5411.

64. White, K. O., E. H. Holt, S. A. Schleusener, and R. F. Calfee, Erbium Laser Propagation in Simulated Atmospheres II. High Resolution Measurement Method, August 1971, ECOM-5398.

65. Waite, R., Field Comparison Between Sling Psychrometer and Meteorological Measuring Set AN/TMQ-22, August 1971, ECOM-5399.

66. Duncan, L. D., Time Series Editing By Generalized Differences, August 1971, ECOM-5400.

67. Reynolds, R. D., Ozone: A Synopsis of its Measurements and Use as an Aemospheric Tracer, August 1971, ECOM-5401.

68. Avara, E. P., and B. T. Miers, Noise Characteristics of Selected Wind and Temperature Data from 30-65 km, August 1971, ECOM-5402.

69. Avara, E. P., and B. T. Miers, Comparison of Linear Trends in Time Series Data Using Regression Analysis, August 1971, ECOM-5403.

70. Miller, W. B., Contributions of Mathematical Structure to the Error Behavior of Rawinsonde Measurements, August 1971, ECOM-5404.

71. Collett, E., Mueller Stokes Matrix Formulation of Fresnel's Equations, August 1971, ECOM-3480.

72. Armendariz, M., and L. J. Rider, Time and Space Correlation and Coherence in the Surface Boundary Layer, September 1971, ECOM-5407.

73. Avara, E. P., Some Effects of Randomization in Hypothesis Testing with Correlated Data, October 1971, ECOM-5408.

74. Randhawa, J. S., Ozone and Temperature Change in the Winter Stratosphere, November 1971, ECOM-5414.

75. Miller, W. B., On Approximation of Mean and Variance-Covariance Matrices of Transformations of Multivariate Random Variables, November 1971, ECOM-5413.

76. Horn, J. D., G. S. Campbell, A. L. Wallis (Capt., USAF), and R. G. McIntyre, Wind Tunnel Simulation and Prototype Studies of Barrier Flow Phenomena, December 1971, ECOM-5416.